

## FACILE PREPARATION OF CuInS<sub>2</sub> THIN FILMS VIA CHEMICAL BATH DEPOSITION AND VACUUM ANNEALING TREATMENT

N. F. WANG<sup>a,\*</sup>, X. M. CHEN<sup>b</sup>

<sup>a</sup>*School of Chemical engineering, Qinghai University, Xining 810016, PR China*

<sup>b</sup>*School of mechanical engineering, Qinghai University, Xining 810016, PR China*

The CuInS<sub>2</sub> thin films have been prepared by chemical bath deposition method and vacuum annealing post-treatment. The deposition solution contained CuSO<sub>4</sub>, In<sub>2</sub>(SO<sub>4</sub>)<sub>3</sub>, CH<sub>3</sub>CSNH<sub>2</sub>, NH<sub>4</sub>NO<sub>3</sub>, and C<sub>6</sub>H<sub>15</sub>NO<sub>3</sub>. The pH value was adjusted to 1.0~1.5 by dilute H<sub>2</sub>SO<sub>4</sub> solution. The films with thickness of 500 nm were obtained by immersing the microscope glass slide substrates into the deposition solution at the temperature of 80 °C for 2 h. The deposited films were annealed in vacuum condition at 520 °C for 30 min. The as-deposited and as-annealed films were examined by SEM, XRD, XRF, XPS, Raman, UV-Vis absorption, and Hall Effect measurements. The as-annealed CuInS<sub>2</sub> is an n-type semiconductor with the optical band gap of 1.78 eV, the major carrier concentration of 5.0×10<sup>14</sup> cm<sup>-3</sup> and the mobility of 4.1 cm<sup>2</sup>/V·s.

(Received April 5, 2018; Accepted July 2, 2018)

**Keywords:** Copper indium disulfide, Thin films, Chemical bath deposition

### 1. Introduction

Chalcopyrite CuInS<sub>2</sub> is a ternary chalcogenide compound which is known to have great potentials as a light absorber layer materials for developing low-cost, low-toxic and high-efficient thin film solar cells. Comparing with other I-III-VI type compound semiconductors, such as CuInSe<sub>2</sub> and Cu(In,Ga)Se<sub>2</sub>, CuInS<sub>2</sub> does not use include toxic and expensive element Se. In the recent years, great progress has been made to develop thin film solar cells based on CuInS<sub>2</sub>[1-7]. Generally, physical vapor deposition (PVD) methods including sputtering[8] and evaporation[9, 10] are widely used to fabricate functional thin films. However, these methods need expensive vacuum equipment, and could hardly be applied to industry relevant area. Therefore, low-cost methods are required for mass production of CuInS<sub>2</sub> thin films. Some works have been carried out to obtain CuInS<sub>2</sub> thin films by electrochemical deposition[11], sol-gel spin-coating[12], spray pyrolysis[7], chemical bath deposition methods[3, 13]. As yet, the preparation of CuInS<sub>2</sub> by chemical bath deposition method and the reaction mechanism have not been well studied. The films synthesized by wet-chemical approaches usually are composed of nanocrystalline or amorphous materials. To achieve the desired crystal structure, annealing post-treatment has been proved to be essential. Most of the annealing processes are carried out in a S or H<sub>2</sub>S atmosphere[10, 14].

In this study, we prepared the precursor thin film by one-step chemical bath deposition method, and n-type CuInS<sub>2</sub> film by vacuum annealing post-treatment. These films were characterized by SEM, XRD, XPS, Raman and UV-Vis absorption measurements. The solution reaction processes of deposition were also analyzed.

### 2. Experimental procedure

We used clean microscope glass slides as substrates. The CuInS<sub>2</sub> thin films were synthesized from a mixed deposition solution containing copper sulfite (CuSO<sub>4</sub>), indium sulfite (In<sub>2</sub>(SO<sub>4</sub>)<sub>3</sub>), thioacetamide (CH<sub>3</sub>CSNH<sub>2</sub>, TAA), ammonium nitrate (NH<sub>4</sub>NO<sub>3</sub>), and triethanolamine (C<sub>6</sub>H<sub>15</sub>NO<sub>3</sub>, TEA). NH<sub>4</sub>NO<sub>3</sub> and TEA acted as the pH buffer of the solution and the complexing

---

\* Corresponding author: nwan754@yahoo.com

agent of  $\text{Cu}^{2+}$  and  $\text{In}^{3+}$ . TAA served as a sulfur source here. In order to obtain a clear and homogeneous precursor solution, the reagents should be mixed in turn. Firstly, 15 ml of 2 M  $\text{NH}_4\text{NO}_3$ , 10 ml of 25 mM  $\text{In}_2(\text{SO}_4)_3$ , 8.4 ml of 120 mM  $\text{CuSO}_4$  were mixed and stirred with high speed for 15 min. Then 1.5 g of liquid TEA was dropped to the stirring solution. It can be observed that the blue precipitation was formed in the solution, which can be ascribed to the complex reaction listed as follows[15]:



Since  $\text{NH}_4\text{NO}_3$  is the salt of a weak base ( $\text{NH}_3 \cdot \text{H}_2\text{O}$ ) and a strong acid ( $\text{HNO}_3$ ), the ionization and hydrolysis reaction happened in the aqueous solution, which make the pH value to be slightly less than 6. In the weak acidic solution, the insoluble  $\text{Cu}(\text{TEA})_n(\text{OH})_2$  was precipitated[16],



After several drops of dilute  $\text{H}_2\text{SO}_4$  were added, the blue precipitation disappeared,



Then, 14 ml of 1 M TAA solution was added slowly with strong stirring, the solution was made up to 100 ml with deionized water. In an aqueous medium, TAA is liable to react with  $\text{H}^+$  and release  $\text{S}^{2-}$  to combine with  $\text{Cu}^{2+}$  and  $\text{In}^{3+}$ ,



The pH was adjusted to 1.0~1.5 with dilute  $\text{H}_2\text{SO}_4$  solution. The bath temperature was controlled to be 80 °C. Within about 10 min, the Cu, In and S ions started to react and combine, and the color of solution changed from light yellow to brown accompanying with the light brown film depositing on the substrate. The sample was taken out from the solution after 2 h of deposition. Then, annealing treatment of film was carried out in a vacuum of  $2.5 \times 10^{-4}$  Pa for 30 min instead of using a sulfur or hydrogen sulphide atmosphere. The heating temperature was raised stepwise (10 min at 230 °C and 320 °C, respectively) up to 520 °C where the sample was annealed for 30 min.

The Surface morphology of thin films were characterized by a JEOL JSM-6460L scanning electron microscopy (SEM) at 20 kV. The bulk composition of samples was measured by X-ray fluorescence spectroscopy (XRF) with a XRF-1800 instrument. The structural properties of the films were examined with a Rigaku TTR3 X-ray diffractometer (XRD) using  $\text{Cu K}_\alpha$  radiation at 50 kV and 200 mA. MicroRaman spectra were recorded on a Reinshaw RM2000 spectrometer (using a 514 nm  $\text{Ar}^+$  laser with a Beam size of  $\sim 5 \mu\text{m}$ ), and obtained at a laser power of 100% (4.7 mW). XPS measurements were carried out on a PHI-5300 type spectrometer at  $1.4 \times 10^{-8}$  torr using  $\text{Al K}_\alpha$  radiation. UV-vis spectra of as-deposited and as-annealed films were characterized using a Cary 5000 UV-Vis-NIR spectrophotometer. Hall coefficient measurement was conducted using an Ecopia HMS-3000 Hall Effect Measurement System.

### 3. Results and discussion

The SEM images of as-deposited and as-annealed thin films are shown in Fig. 1. The as-deposited film exhibits a smooth and uniform surface over the given range of scale, and composed of sphere-like particles. No cracks can be found, which is beneficial for its photovoltaic applications. After annealing, the film becomes denser, and the particles grow larger. XRF analysis shows that the thicknesses of films are about 500 nm. The bulk compositions of films were measured by XRF, listed in Table 1. According to the formula proposed by Guillen et al.[17], the composition data of  $\text{Cu}_a\text{In}_b\text{S}_c$  compound can be translated into deviation from molecularity ( $\Delta m$ ) and deviation from stoichiometry ( $\Delta s$ ) to take more precisely into account the role of the deviation from the ideal composition. Definitions of  $\Delta m$  and  $\Delta s$  are[17]

$$\Delta m = (a-b)/b, \Delta s = (2c-a-3b)/(a+3b) \quad (8)$$

The as-deposited film with atomic ration of Cu: In: S = 1: 1.67: 2.25, and  $\Delta m = -0.40 < 0$ ,  $\Delta s = -0.25 < 0$ , is correlated with an excess of indium element and a deficiency of sulfur element. After annealing, the film with atomic ration of Cu: In: S = 1: 0.56: 0.63, presented values  $\Delta m = 0.78 > 0$ ,  $\Delta s = -0.53 < 0$ , indicating an excess of copper and a deficiency of sulfur. It can be concluded that parts of indium and sulfur elements vaporized during the vacuum annealing process.

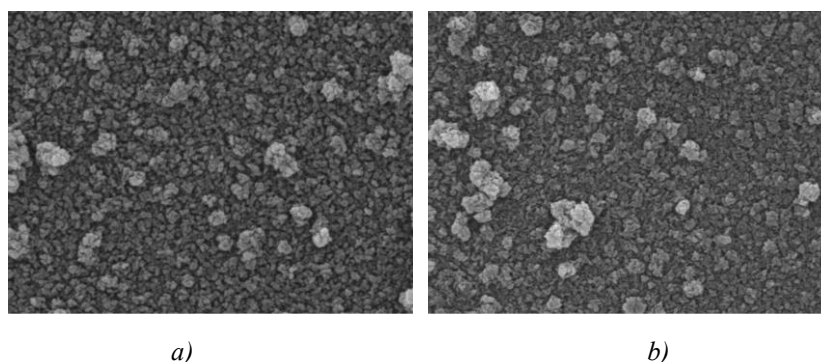
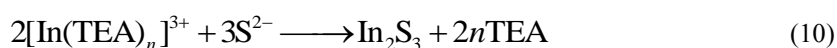
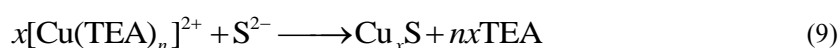


Fig. 1. SEM images of thin films: (a) as-deposited film; (b) as-annealed film.

Table 1. Composition of as-deposited and as-annealed thin films.

samples	Cu (at%)	In (at%)	S (at%)	Cu/In	S/Cu
as-deposited	20.31	34.00	45.69	0.60	2.25
as-annealed	45.62	25.70	28.68	1.78	0.63

Fig. 2 shows XRD patterns of as prepared and as-annealed thin films. The amorphous peaks of soda-lime glass were erased from the spectra. It is observed that, the as-deposited film is composed of two phases: the tetragonal  $\text{In}_2\text{S}_3$  (space group:  $I41/amd$ , PDF#21-0413) and trigonal  $\text{Cu}_x\text{S}$  (space group:  $R\bar{3}m$ , PDF#33-0491). Therefore, the deposition process can be described as follows:



After annealing, the peaks of  $\text{Cu}_x\text{S}$  and  $\text{In}_2\text{S}_3$  phases disappeared. We found the XRD pattern exhibited peaks at  $2\theta = 27.85^\circ$ ,  $46.32^\circ$ , and  $54.80^\circ$ , which correspond to the (112),

(204/220), and (116/312) crystal planes of chalcopyrite  $\text{CuInS}_2$  phase. The combination reaction between  $\text{Cu}_x\text{S}$  and  $\text{In}_2\text{S}_3$  phases can be expressed as follow:

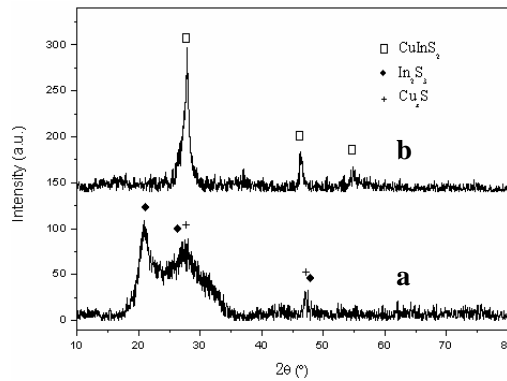


Fig. 2. XRD diffraction patterns of thin films: (a) as-deposited; (b) as-annealed.

The XPS measurement has been carried out to obtain element compositional and combining information of the annealed  $\text{CuInS}_2$  film. A survey spectrum was shown in Fig. 3a, indicated the presence of Cu, In and S, as well as O and C impurity. The content of C and O should be attributed to the adventitious C on the examined sample and the adsorption of  $\text{O}_2$  and  $\text{CO}_2$  from air. High-resolution spectra were taken for the Cu 2p, In 3d and S 2p regions. The binding energies of Cu  $2p_{3/2}$ , Cu  $2p_{1/2}$ , In  $3d_{5/2}$ , In  $3d_{3/2}$ , S  $2p_{3/2}$  and S  $2p_{1/2}$  were labeled on the core level spectra in Fig. 3b~3d, which were in well agreement with the literature values[18].

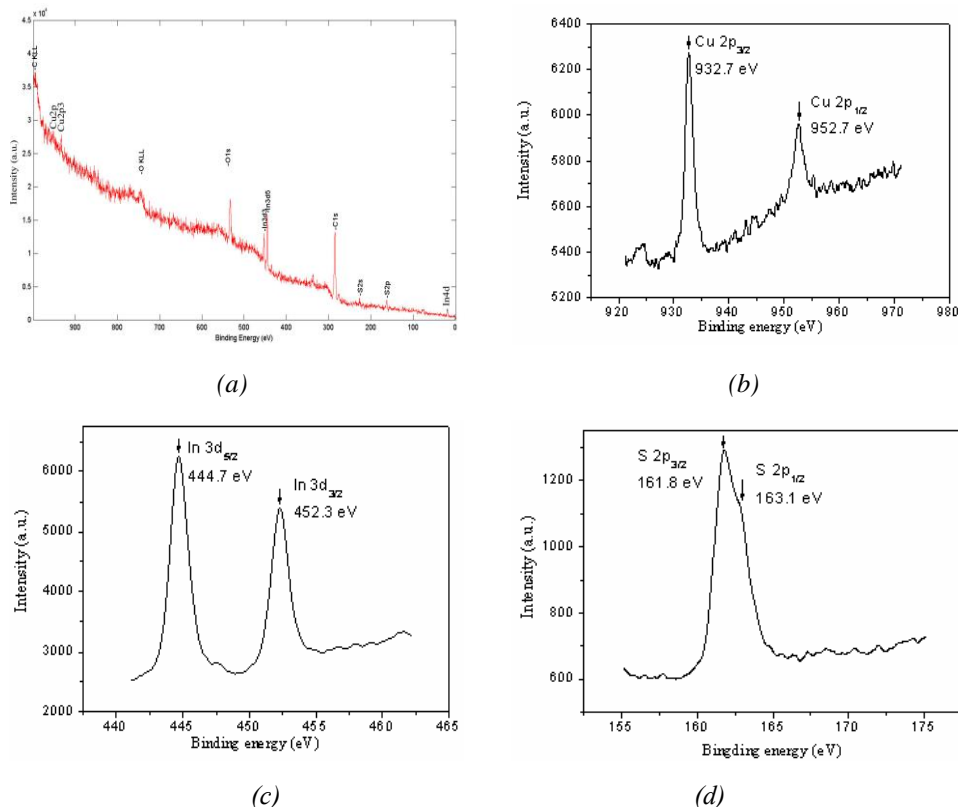


Fig. 3. XPS spectra of as-annealed  $\text{CuInS}_2$  thin films: (a) survey spectrum; (b) ~ (d) core level spectra of Cu 2p, In 3d, and S 2p, respectively.

Fig. 4 shows the Raman spectra of as-deposited and as-annealed thin films. From the spectrum of as-deposited film, only one wide peak centered at the wave number of  $310\text{ cm}^{-1}$  was observed, which can be attributed to the nanostructured  $\text{Cu}_x\text{S}$  and  $\text{In}_2\text{S}_3$  phase. On the other hand, the as-annealed Raman spectrum showed two characteristic peak of chalcopyrite  $\text{CuInS}_2$  phase at  $294\text{ cm}^{-1}$  and  $336\text{ cm}^{-1}$ , which can be assigned to  $A_1$  and  $B_2$  modes, respectively[19].

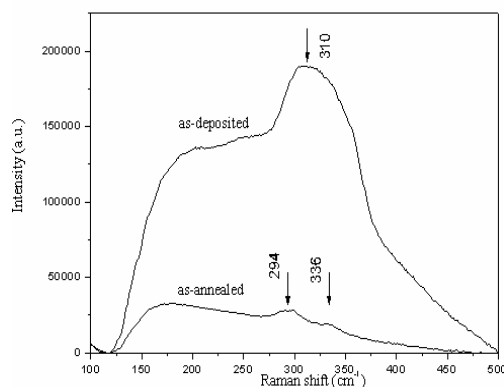


Fig. 4. Raman spectra of as-deposited and as-annealed thin films.

Fig. 5a shows the absorbance spectrum of as-annealed  $\text{CuInS}_2$  thin films. It is well known that absorption coefficient ( $\alpha$ ) of semiconductor materials is related to the incident photon energy ( $h\nu$ ) by the following equation[20-22]:

$$(\alpha h\nu) = A(h\nu - E_g)^m \quad (12)$$

where  $A$  is a constant,  $E_g$  is the optical band gap of semiconductor,  $m$  is taken as  $1/2$  for direct band gap materials or  $2$  for indirect band gap materials.  $\text{CuInS}_2$  is a direct band gap semiconductor,  $m=1/2$ . The optical band gap  $E_g$  can be obtained from the plot of  $(\alpha h\nu)^2$  versus  $h\nu$ , as shown in Fig. 5b. Extrapolating the straight line portion of the plot of  $(\alpha h\nu)^2$  against  $h\nu$  to the energy axis for  $(\alpha h\nu)^2=0$  give optical band gap of the semiconductor. The optical band gap of as-annealed  $\text{CuInS}_2$  thin film is about  $1.78\text{ eV}$ , which is lightly larger than the bulk theoretical value of  $1.50\text{ eV}$ . The might be ascribed to the blue shift of the absorption edge due to the nanostructured  $\text{CuInS}_2$  grains. The electrical properties of as-annealed film also have been measured. It shows that the conductivity of film is n-type, with the major carrier concentration of  $5.0 \times 10^{14}\text{ cm}^{-3}$  and the mobility of  $4.1\text{ cm}^2/\text{V}\cdot\text{s}$ .

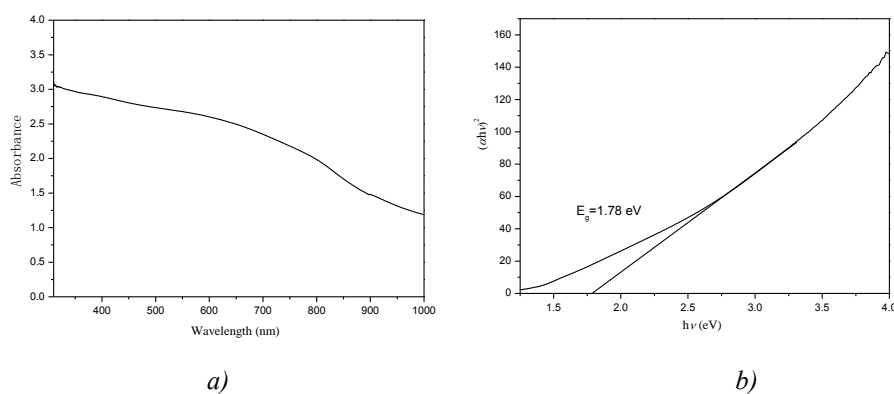


Fig. 5. (a) UV-Vis absorbance spectrum; (b)  $(\alpha h\nu)^2$  versus  $h\nu$  of  $\text{CuInS}_2$  thin films.

#### 4. Conclusions

The CuInS<sub>2</sub> thin films have been prepared by chemical bath deposition method and vacuum annealing post-treatment. The films are densely compacted and suitable for photovoltaic applications.

The as-deposited precursor films are composed of In<sub>2</sub>S<sub>3</sub> and Cu<sub>x</sub>S phases. After vacuum annealing, single-phased chalcopyrite CuInS<sub>2</sub> thin films can be formed, during which In and S elements are partly evaporated and the composition of films change from In-rich to Cu-rich. The as-annealed CuInS<sub>2</sub> is an n-type semiconductor with the optical band gap of 1.78 eV, the major carrier concentration of  $5.0 \times 10^{14} \text{ cm}^{-3}$  and the mobility of  $4.1 \text{ cm}^2/\text{V}\cdot\text{s}$ .

#### Acknowledgements

This work has been financially supported by the research project of chemical engineering college, Qinghai University.

#### References

- [1] X. H. Xu, F. Wang, J. J. Liu, K. C. Park, M. Fujishige, *Solar Energy Materials and Solar Cells* **95**(2), 791(2011).
- [2] H. Z. Zhong, S. S. Lo, T. Mirkovic, Y. C. Li, Y. Q. Ding, Y. F. Li, G. D. Scholes, *Acs Nano* **4**(9), 5253(2010).
- [3] X. H. Xua, F. Wang, J. J. Liu, J. Ji, *Electrochimica Acta* **55**(15), 4428(2010).
- [4] J. Xu, C. S. Lee, Y. B. Tang, X. Chen, Z. H. Chen, W. J. Zhang, S. T. Lee, W. X. Zhang, Z. H. Yang, *Acs Nano* **4**(4), 1845(2010).
- [5] R. Ishikawa, T. Oya, T. Yamada, T. Nomoto, N. Tsuboi, *Thin Solid Films* **634**, 1(2017).
- [6] B. Huang, R. Xu, L. Zhang, Y. Yuan, C. Lu, Y. Cui, J. Zhang, *Journal of Materials Chemistry C* **46**(5), 12151(2017).
- [7] M. A. Hassan, M. Mujahid, L. S. Woei, L. H. Wong, *Materials Research Express* **5**(3), 035506 (2018).
- [8] S. Seeger, K. Ellmer, *Thin Solid Films* **517**(10), 3143 (2009).
- [9] N. Khemiri, M. Kanzari, *Journal of Materials Science* **44**, 4743(2009).
- [10] J. K. Larsen, J. Keller, O. Lundberg, T. Jarmar, L. Riekehr, J. J. S. Scragg, C. Platzer-Bjorkman, *IEEE Journal of Photovoltaics* **8**(2), 604(2018).
- [11] S. M. Lee, S. Ikeda, T. Yagi, T. Harada, A. Ennaoui, M. Matsumura, *Physical Chemistry Chemical Physics* **13**(14), 6662 (2011).
- [12] L. Oliveira, T. Todorov, E. Chassaing, D. LinCot, J. Carda, P. Escrivano, *Thin Solid Films* **517**(7), 2272 (2009).
- [13] S. Jindal, S. M. Giripunje, S. B. Kondawar, P. Koinkar, *Journal of Physics and Chemistry of Solids* **114**, 163 (2018).
- [14] D. Y. Lee, J. Kim, *Solar Energy Materials and Solar Cells* **95**(1), 245(2011).
- [15] S. Chavhan, R. Sharma, *Journal of Physics and Chemistry of Solids* **67**(4), 767(2006).
- [16] J. F. Fisher, J. L. Hall, *Analytical Chemistry* **35**(8), 1094(1962).
- [17] C. Guillen, J. Herrero, *Journal of the Electrochemical Society* **141**(1), 225 (1994).
- [18] R. Sharma, S. Shim, R. S. Mane, T. Ganesh, A. Ghule, G. Cai, D. H. Ham, S. K. Min, W. Lee, S. H. Han, *Materials Chemistry and Physics* **116**(1), 28(2009).
- [19] D. Y. Lee, J. Kim, *Thin Solid Films* **518**(2), 6537(2010).
- [20] D. Dwyer, R. Sun, H. Efsthadiadis, P. Haldar, *Physica Status Solidi a-Applications and Materials Science* **207**(10), 2272 (2010).
- [21] K. R. Murali, A. Shanmughavel, K. Srinivasan, *Chalcogenide Letters* **7**(5), 385 (2010).
- [22] M. B. Rabeh, N. Chaglabou, M. Kanzari, *Chalcogenide Letters* **6**(2), 83(2009).